Earth System
Dynamics
Discussions

Open Access

Global warming projections derived from an observation-based minimal model

K. Rypdal

Department of Mathematics and Statistics, UiT The Arctic University of Norway, Tromsø, Norway

Correspondence to: K. Rypdal (kristoffer.rypdal@uit.no)

Discussion Paper | Discussion Paper | Discussion Paper | Discussion Paper |

ESDD

6, 1789–1813, 2015

Inertia in the climate response

K. Rypdal

Title Page

Abstract | Introduction

Conclusions | References

Tables | Figures

◄ | ►►

◄ | ►

Back | Close

Full Screen / Esc

Printer-friendly Version

Interactive Discussion

Abstract

A simple conceptual model for the global mean surface temperature (GMST) response to CO_2 emissions is presented and analysed. It consists of linear long-memory models for the GMST anomaly response ΔT to radiative forcing and atmospheric CO_2-concentration response ΔC to emission rate. The responses are connected by the standard logarithmic relation between CO_2 concentration and its radiative forcing. The model depends on two sensitivity parameters, α_T and α_C, and two "inertia parameters", the memory exponents β_T and β_C. Based on observation data, and constrained by results from the Climate Model Intercomparison Project Phase 5 (CMIP5), the likely values and range of these parameters are estimated, and projections of future warming for the parameters in this range are computed for various idealised, but instructive, emission scenarios. It is concluded that delays in the initiation of an effective global emission reduction regime is the single most important factor that influences the magnitude of global warming over the next two centuries. The main value of this study is the simplicity and transparency of the conceptual model, which makes it a useful tool for communicating the issue to non-climate scientists, students, policy-makers, and the general public.

1 Introduction

In spite of five comprehensive reports from the Intergovernment Panel on Climate Change (IPCC) the perception of the threat of global warming to society remains highly diverse among the general public, decision makers, and the broad community of scientists. This is in stark contrast to the general opinion among those who define themselves as climate scientists, where some studies suggest that as much as 97 % recognise human activity as a main driver of dangerous global change (Anderegg et al., 2010; Cook et al., 2013). What distinguishes the climate science community from other scientists is the strong reliance among climate scientists on complex Earth System

Models (ESMs), that is, on Atmospheric-Ocean General Circulation Models (AOGCMs) coupled to models that include biogeochemistry and cryosphere dynamics. The general skepticism against this "model science" is not hard to understand. Models are complex beyond comprehension, different models are not independent but consist of many common modules, and parametrisations are empirical to an extent that makes it legitimate to question whether models are "massaged" to fit observations. The important point here is not whether this perception of climate modelling is correct or fair, but that the skepticism exists, and in many cases cannot be discarded as irrational.

The latest IPCC report from Work Group I on the climate system (IPCC AR5 WG1, 2013) contains a summary for policy makers that describes findings from observations and model studies which many physical scientists find unconvincing, and is not very easy read for the general public. The unconvincing part is the above mentioned reliance on complex computer models. Most scientists want to understand and to be convinced by simple fundamental principles matched against clear-cut observations. And decision makers and the informed layman want to see simple, clear alternatives for the future; not a myriad of incomprehensible scenarios labelled by meaningless acronyms.

From the Co-Chair of Work Group I a very readable and important paper on the "The Closing Door of Climate Targets" (Stocker, 2013) was published alongside the IPCC AR5 report, intended to demonstrate that as mitigation is delayed, climate targets formulated in international agreements become unattainable. The results were based on the physical assumption of a linear relationship between the cumulated carbon emissions and peak global warming in scenarios where the cumulative emission is bounded. This relationship, and the constant of proportionality, were justified empirically from numerical experiments performed on a large number of ESMs which incorporate the global carbon cycle (Allen et al., 2009; Matthews et al., 2009). Some readers, however, will find it unsatisfactory that they have to "believe" the models in order to accept the conclusion of the paper. As a former plasma physicist, who only relatively recently has taken up research in Earth-system dynamics and climate science, I am often confronted with question from former colleagues of the type: "For half

Printer-friendly Version

Interactive Discussion

a century we have tried to model the transport properties of a magnetically confined plasma for controlled thermonuclear fusion, and we still haven't succeeded very well, even though the physical system is infinitely simpler than the climate. Why do you think these horrendously complex climate models perform any better?"

5 　A major motivation for the present paper is to find ways to communicate with, and gain support from, the scientists who ask such questions. I do this by deriving results similar to those obtained in Stocker (2013) in a more transparent manner, and without resorting to complex ESMs as the primary justification. The underlying assumptions are justified from observations, although supporting evidence from AOGCMs are also dis-

10 cussed. The conceptual models of the temperature and atmospheric carbon response are linear and simple enough to be understood by anyone with some background in elementary calculus and ordinary differential equations. The scenarios explored are idealised and the results presented in figures that should be comprehensible for readers without training in mathematics or physical sciences.

15 　Section 2 describes and justifies the conceptual model. In Sect. 3, I present projections for atmospheric CO_2 concentration and GMST for some idealised CO_2 emission scenarios, one which is very close to the "business as usual" Representative Concentration Pathway 8.5 (RCP8.5) scenario employed by the IPPC, and others which represent systematic emission reduction initiated at different times in the future. Here I

20 also discuss policy implications that may follow from these projections, and in Sect. 4, I summarise and conclude. The Supplement contains data files and a link to well-documented *Mathematica* notebook with routines that allow readers to replicate and extend all results presented in the paper.

2　The conceptual model

25 A closed model for the evolution of the global mean surface temperature (GMST) could consist of (i) a model for the GMST-anomaly response $\Delta T(t)$ to radiative forcing $F(t)$, (ii), a model for the evolution of $\Delta C(t)$, given the CO_2 emission history $R(t)$,

Full Screen / Esc

Printer-friendly Version

Interactive Discussion

and (iii) a well established constitutive relation between $F(t)$ and $\Delta C(t)$. In this paper I propose extremely simple, linear models for the GMST-response (i) and the CO_2-concentration response (ii). Each depends on two parameters characterising the strength and the inertia (memory) of the response, respectively. In order to keep the model sufficiently simple for a reader to be able to trace the connection between driver and response, and the effect of variation of model parameters, I have made major simplifying assumptions. One is to neglect all other radiative forcing than CO_2. Although the main reason for this is to maintain simplicity, it is justified by forcing estimates that conclude the the non-CO_2 contributions tend to cancel over the industrial period (IPCC AR5 WG1, 2013). Other important simplifications are linearity and stationarity:

– Linearity: global temperature has been found to respond quite linearly to forcing in general circulation models (Meehl et al., 2004), and as long as the climate system is far from a major tipping point, this linearity may also pertain to the response of atmospheric CO_2 content to emissions. The effect of space-time non-linearity on variability on smaller than global scale ("turbulence") is taken into account through a linear response function of power-law form that makes the system respond by a scale-invariant stochastic process to a white-noise driver.

– Stationarity: the response functions are assumed to be translation invariant, i.e. $G(t, t') = G(t - t')$. This means that the GMST and the CO_2 concentration respond the same way in a future climate as they do now. This assumption may be particularly wrong for the CO_2 concentration, where e.g. saturation effects in the ocean mixed layer and the land biosphere may reduce fluxes in a future climate. It also neglects the coupling between sea surface temperature and the CO_2 flux, which will reduce the flux into the ocean in a warmer climate. However, such effects can be taken into account in a rudimentary fashion by introducing several response time scales, for instance through a power-law tail in the response function.

2.1 The temperature response

The simplest physics-based model of the GMST-response is the zero-dimensional, lin-earised energy balance model (EBM);

$$\frac{d}{dt}\Delta T = -\frac{1}{\tau_T}\Delta T + \frac{S}{\tau_T}F. \tag{1}$$

Here τ_T is the time constant for relaxation of the temperature anomaly, and S is the climate sensitivity. The model is often denoted the Budyko–Sellers model and first proposed by Budyko (1969) and Sellers (1969). A simple derivation can be found in Rypdal (2012), where it is also pointed out that it is impossible to find a single time constant that describes adequately the response to forcing on all time scales. This model is not only used for reproducing the global temperature to known (deterministic) forcing, but can also be formulated as a stochastic differential equation by introducing a noise component to the forcing $F(t)$, representing the stochastic energy flux from at-mospheric weather systems to the ocean and land surface (Rypdal and Rypdal, 2014). The solution to this equation can be written as a convolution integral

$$\Delta T(t) = \int_0^t G_T(t - t')F(t')\,dt', \tag{2}$$

with an exponential response function

$$G_T(t) = (S/\tau_T)\exp(-t/\tau_T). \tag{3}$$

The temperature response to a purely stochastic forcing, i.e. $F(t)$ is represented as a Gaussian white noise, is an Ornstein–Uhlenbeck stochastic process. In discrete time, this corresponds to a first-order autoregressive (AR(1)) process. If Eq. (1) provides an adequate description, with $F(t)$ separated into a deterministic and a white-noise com-ponent, then the residual obtained after subtracting the deterministic response from

Inertia in the climate response

K. Rypdal

Title Page

Abstract | Introduction

Conclusions | References

Tables | Figures

◀◀ | ▶▶

◀ | ▶

Back | Close

Full Screen / Esc

Printer-friendly Version

Interactive Discussion

the observed annual GMST record should be a realisation of an AR(1) process. The time constant and the climate sensitivity can be determined by a maximum-likelihood estimation, and in Rypdal and Rypdal (2014) they were estimated to $\tau \approx 4.3\,\mathrm{yr}$, and $S \approx 0.32\,\mathrm{km^2\,W^{-1}}$. However, the sensitivity obtained is lower than obtained from climate models, the fast response to volcanic eruptions is higher than in the observed record, and the residual does not conform well with an AR(1) process. Rypdal and Rypdal (2014) demonstrated that the residual is better described by a model for persistent, fractional Gaussian noise (fGn). Such a noise can be produced by Eq. (2) if the exponential response function is replaced by a power-law function

$$G_T(t) = \alpha_T t^{\beta_T/2-1}, \tag{4}$$

where the memory exponent β_T is in the interval $0 < \beta_T < 1$. It can be shown that this process has a power spectral density on the form $\sim f^{-\beta_T}$, where f is the frequency (Beran, 1994). Hence, $\beta_T = 0$ corresponds to white noise, while increasing β_T signifies increasing degree of memory (or persistence) in the process. In this response model it replaces the time constant τ_T of the simple EBM. The parameter α_T replaces the climate sensitivity S. In Rypdal and Rypdal (2014) the magnitude of the parameters α_T and β_T were estimated from the instrumental GMST record, revealing rather strong persistence, $\beta_T \approx 0.75$. Similar values were also found in multiproxy data for the Northern Hemisphere, and in Østvand et al. (2014) they were found in data from a number of millennium-long AOGCM simulations. The long power-law tail in the response function may be interpreted as an effect of thermal exchange between the surface (e.g. the ocean mixed layer) and other components of the climate system with higher heat capacity (e.g. the deep ocean). A two-layer ocean energy balance model yields for instance a response function with two exponentials with different time constant. In Geoffroy et al. (2013) such a two-layer model was compared to transient simulations of AOGCMs following an abrupt increase in CO_2 forcing, and the two time constants estimated from these data were typically 1–2 years and 1–2 centuries, respectively. In Rypdal et al. (2015) it was shown that a power-law response provides an even bet-

ter fit to the tail of the transient AOGCM-solutions, but the memory exponent is lower ($\beta_T \approx 0.35$) than found from the residuals in observations and AOGCM simulations with historical forcing. One way of reconciling these conflicting results is to assume that the forcing noise is not white, but rather a persistent noise which gives a contribution to the β_T observed in the residuals. On the other hand, it will be pointed out in Sect. 3 that the Computer Model Intercomparison Project Phase 5 (CMIP5) in the RCP8.5 CO_2 concentration scenario yields results consistent with $\beta_T = 0.75$. Since this implies some uncertainty with respect to the correct value of β_T for the temperature response I shall in Sect. 3 present projections for the values $\beta_T = 0.35$ and $\beta_T = 0.75$, assuming that β_T is likely within this interval but probably closer to the higher value.

The significance of the inertia (memory) in the temperature response for GMST projections is illustrated in Fig. 1. Panel a shows the estimated GMST response to a forcing scenario consisting of the anthropogenic forcing in the period AD 1880–2010 as presented in Hansen et al. (2011), linearly projected to AD 2200 with the same mean growth rate as the the RCP8.5 scenario in the period AD 2010–2100 (Meinshausen et al., 2011), and is shown as the blue curve in Fig. 1b. The blue and red curves in Fig. 1a are the responses according to the power-law response models with $\beta_T = 0.35$, and $\beta_T = 0.75$, respectively. The projection for an instant response ($\tau_T \to 0$, leading to $\Delta T(t) \to SF(t)$) is also shown as the limit of zero inertia. Also shown as a light blue curve is the instrumental GMST record as given by Brohan et al. (2006). These projections have been obtained by computing the integral $\int_0^t \alpha_T (t - t')^{(\beta_T/2-1)} F(t') \, dt'$ with the specified β_T and then estimating α_T by regressing to the observed GMST record for the period AD 1880–2010. The climate sensitivity S for the instantaneous response has also been found by regressing $SF(t)$ to the instrumental data, and is found to be $S \approx 0.48 \, \text{km}^2 \, \text{W}^{-1}$, which corresponds to 1.8 K for a doubling of CO_2 concentration. The rising warming projected for increasing β_T is a manifestation of the thermal inertia in parts of the climate system with high heat capacity that exchange heat with the surface, and makes the surface temperature respond more slowly. The higher surface warming

in the distant future due to this inertia is a manifestation of "the warming in the pipeline" (Hansen et al., 2011; Rypdal, 2012).

The blue forcing path shown in Fig. 1b is an idealised "business as usual" (BAU) scenario. Beyond AD 2100 there is every reason to believe that there will be a saturation of the rising trend, even in the absence of active mitigation policies. In the RCP8.5 this takes place gradually during the 22nd and first half of the 23rd century. This figure also shows some idealised scenarios where the BAU is modified by mitigation action. One possible type of action is the sudden reduction of emission that will stabilise the forcing at the level at the time of action. In the real world such an action from one year to another is not possible, but it may be considered an approximation of certain annual reduction over a period of a decade. For instance, 40 % emission reduction can be achieved by annual emission reduction of 5 % over a decade. In Fig. 1b forcing scenarios for this type of mitigation action are illustrated for three different years of onset of the action; AD 2030, 2070, and 2110. The year 2030 gives the world fifteen years to prepare the action. Year 2070 leaves the problem to those who are born today, i.e. to the next generation. Year 2110 leaves it to unborn generations.

The GMST projections for these scenarios are shown in Fig. 1c and d for the lower and higher memory exponents β_T. Under the low-inertia assumption in the temperature response ($\beta_T = 0.35$) the unmitigated forcing scenario in Fig. 1a yields approximately two degree of warming every 40 years throughout the 21st century, and even higher rate of warming in the 22nd century. After stabilisation of the atmospheric CO_2 concentration, the temperature will continue to rise about one degree Celcius by the year AD 2200, independent on when this stabilisation takes place. This one degree of additional warming is the "warming in the pipeline." Under the high-inertia assumption ($\beta_T = 0.75$) the warming rate is approximately 30 % higher, and the warming in the pipeline is about a 100 % higher. The high-inertia projection with mitigation action in AD 2110 is very close to the multimodel mean RCP8.5 projection (Meinshausen et al., 2011), suggesting some consistency between this simple global temperature response model and the models employed by the IPCC in the CMIP5 project.

Figure 1c and d suggest that the two-degree Celcius target is unlikely to be attained by rapid stabilisation of atmospheric CO_2 concentration, if this action is started later than AD 2030. If radical action is postponed until the GMST has passed the two-degree limit, it is likely that the global temperature will exceed three degrees by AD 2100, and if action is postponed till the end of this century our descendants may experience a world that is 5–8 °C warmer than before industrialisation.

2.2 The atmospheric CO_2 response

The dominant driver of climate change throughout the 20th century and beyond is anthropogenic radiative forcing, and in the 21st century, CO_2 forcing is expected to be the main anthropogenic driver. However, while AOGCMs traditionally have been driven by prescribing the atmospheric CO_2 concentration, the policy relevant quantity is the CO_2 emission rate. The main factor that determines future CO_2 forcing in a given emission scenario is the rate at which CO_2 is washed out of the atmosphere. This is where the carbon-cycle models incorporated in the ESMs become important. The model uncertainty is high, but suggest the existence of a hierarchy of time scales, just as we have found in the temperature response (Joos et al., 2013). This hierarchy is not immediately apparent from the instrumental data records, but there is some indirect evidence, as will be demonstrated below. However, let us first consider a primitive model with only one response time scale, analogous to the simple EBM given by Eq. (1) for the surface temperature. In this model we assume that the Carbon flux out of the atmosphere is proportional to the anomaly ΔC of atmospheric Carbon content relative to the preindustrial concentration C_0. This assumption follows from a Taylor expansion to first order of the Carbon flux $I(\Delta C) = (1/\tau_C)\Delta C + \ldots$ around the preindustrial equilibrium $I(C_0) = 0$. The primitive equation for this perturbation is then

$$\frac{\mathrm{d}}{\mathrm{d}t}\Delta C = -\frac{1}{\tau_C}\Delta C + R, \tag{5}$$

where τ_C is the time constant for relaxation of CO_2 concentration to the preindustrial equilibrium. A first-order estimate of τ_C can be made from the estimates of the global carbon budget (Le Quéré et al., 2015). The annual carbon emission in the period 1960–2010 grew almost linearly from 4 to $11\,\mathrm{Gt\,C\,yr^{-1}}$. We can solve Eq. (5) for this period with $R = [4 + (7/50)]\,t\,\mathrm{Gt\,C\,yr^{-1}}$ in terms of τ_C and the initial atmospheric Carbon inventory anomaly, ΔC_{1960}. The conversion factor from concentration in ppm to Gt C in total Carbon content is 2.12 (Le Quéré et al., 2015), which yields $\Delta C_{1960} = (315 - 280) \times 2.12 \approx 74\,\mathrm{Gt\,C}$ if we assume a CO_2 concentration of 315 ppm in 1960 and preindustrial concentration 280 ppm. The preindustrial Carbon content, corresponding to 280 ppm, was $C_0 \approx 594\,\mathrm{Gt\,C}$. This solution reproduces very well the observed evolution of the atmospheric CO_2 content in this period if one chooses $\tau_C = 33\,\mathrm{yr}$, as shown in Fig. 2a, and suggests that $\Delta C(t)$ is described by the response function,

$$\Delta G_C(t) = (r/\tau_C)\Delta C(t)\exp[-t/\tau_C]. \tag{6}$$

A calibration factor r has been introduced here because this response function is certainly too simplistic. For instance, Taylor expansion to first order does not take into account saturation of carbon flux into the ocean, which will invoke a much longer response time governed by biogeochemical processes of transport of Carbon from the mixed layer into the deep ocean. If we fix τ_C at value higher than 33 years, r can be estimated by a simple, linear regression to the historic CO_2 concentration record. For $\tau_C = 33\,\mathrm{yr}$ such regression yields of course $r \approx 1$, but for $r \geq 300\,\mathrm{yr}$ it yields $r \approx 0.5$. This means that the "effective emission rate" in Eq. (5) is is reduced to $rR(t)$. The natural interpretation is that approximately half of the emitted CO_2 is almost instantly removed from the atmosphere and the remainder has a lifetime of centuries, maybe millennia, i.e., that the response occurs on one fast and one slow time scale. Model studies, however, may suggest a hierarchy of time scales for the CO_2 concentration response. The large model comparison study of Joos et al. (2013) reveals a non-exponential tail in the response to a pulse of emitted CO_2. Figure 2b shows that the multimodel mean is very

well approximated by a power-law of the form

$$G_C(t) = \alpha_C t^{\beta_C/2-1}, \tag{7}$$

with $\beta_C \approx 1.6$. This power-law response suggests the simple, linear response model

$$\Delta C(t) = \int_0^t G_C(t - t')R(t')\,dt', \tag{8}$$

where the emission rate $R(t)$ may contain a stochastic contribution, giving rise to a stochastic component to ΔC. This stochastic component of ΔC is shown in Fig. 2c, as the residual obtained after subtracting a quadratic, polynomial fit to the Muana Lua record (the anthropogenic trend) and the seasonal variation. The power spectral density of this residual is shown in Fig. 2c, and indicates that the spectrum is consistent with a power law with spectral index $\beta_C \approx 1.6$ on time scales longer than a few years. The short duration of the record precludes *accurate* estimates of β_C from the spectrum, but it lends some support to the power-law response model with memory exponent in the range $1 < \beta_C < 2$.

2.3 The constitutive relation

A simple relation between CO_2 concentration anomaly and its radiative forcing is (Myhre et al., 1998),

$$F = 5.35 \ln(1 + \Delta C/C_0) \ \text{W\,m}^{-2}. \tag{9}$$

Given an emission scenario $R(t)$, Eq. (8) can be used to compute $\Delta C(t)$ and from Eq. (9) one obtains $F(t)$. Finally this forcing is applied in Eq. (2) to compute $\Delta T(t)$.

3   Projections

3.1   Emission scenarios

Figure 3 shows six different CO_2 emission scenarios. The baseline (unmitigated) scenario is the blue curve, which is an exponential fitted through the actual emission rates in 1960 and in AD 2010. Interpreted as CO_2 equivalents of all well-mixed greenhouse gases it is close to the RCP8.5 emission scenario up till 2070, but is higher after this time, since the RCP8.5 emission rates saturate between 2070 and 2100. At AD 2030, 2070, and 2110 two types of mitigation action are considered. One where emissions are reduced by 1 % per yr (50 % reduction over 70 years) and one with 5 % per yr (50 % reduction over 13.5 years). The former is considered politically and economically feasible (Stern, 2007), the latter is at the limit of what is possible without total disruption of the world economy (den Elzen et al., 2007). The scenarios are similar to those considered by Stocker (2013), although they are prescribed from AD 1880, not from the present day. This is important for the response models employed here, since inertia (long memory) effects from the historical period of global emissions and warming influence the future projections.

3.2   Projections of CO_2 concentration

Atmospheric CO_2 concentrations $\Delta C(t)$ for the emission scenarios described in Fig. 3 are shown in Fig. 4. They are computed from Eq. (8), using the emission scenarios of Fig. 3, and subsequently estimating r by regressing to the historic $\Delta C(t)$ record. Figure 4a shows the concentration scenarios estimated from the exponential response kernel with $\tau_C = 33$ yr. Few climate scientists believe that atmospheric, anthropogenic CO_2 are eliminated as fast as this, but it is interesting to examine, since this is still claimed by some "global warming skeptics" (Solomon, 2008). In Fig. 4b and d the same scenarios are shown, assuming $\tau_C = 300$ yr and $\tau_C = \infty$, respectively. Here $r \approx$ 0.5, i.e. 50 % of the emitted CO_2 immediately removed from the atmosphere and the

rest decaying exponentially with e-folding time τ_C. Figure 4c employs the power-law response kernel with $\beta_C = 1.6$. Figure 4b and c are almost identical, indicating that immediate removal of half of the emitted CO_2, followed by an exponential decay with $\tau_C = 300$ yr, has almost the same effect as a long-memory (power-law) response with $\beta_C = 1.6$.

The unmitigated concentration scenarios (blue curves) are almost the same in all models, and are very similar to the RCP8.5 scenario up to AD 2100. This is because the calibration factor r adjusts the scenario to fit the historic record. However, the evolution after mitigation action has started varies considerably between the models. The overly optimistic model in Fig. 4a, where $\tau_C = 33$ yr, predicts that the concentration starts declining a few decades after emission reduction has started, whereas in the other scenarios concentration continues to rise beyond AD 2200 in the 1 % reduction scenarios. The scenario corresponding to the red full curves in Fig. 4b or c correspond closely to the full RCP8.5 scenario.

3.3 Projections of the GMST

The forcing $F(t)$ for the various concentration scenarios is computed from Eq. (9), and inserted into Eq. (2) to obtain the temperature evolution. Figure 5 shows results for the concentration scenarios obtained from the exponential CO_2 concentration model with $\tau_C = 33$ yr and the power-law model with $\beta_C = 1.6$, considering these to represent low- and high-inertia ends of the CO_2 response. For each of these cases, low- and high-inertia ends ($\beta_T = 0.35$ and $\beta_T = 0.75$) of the GMST response are presented in the figure.

The projections for the high-inertia combination $\beta_C = 1.6$, $\beta_T = 0.75$ shown in Fig. 5d is the one that is most consistent with multi-model CMIP5 projections in the RCP8.5 scenario. As mentioned in Sect. 3.2, the red curve in Fig. 4c is close to the RCP8.5 CO_2-concentration pathway, and the corresponding GMST response shown by the red curve in Fig. 5d is close to the multimodel-mean GMST response given in Fig. 6 of Meinshausen et al. (2011). The high-end inertia ($\beta_T = 0.75$) for GMST response is also

more consistent with analysis of instrumental records and multiproxy reconstructions of GMST (Rypdal et al., 2015) and millennium-long simulations of intermediate and high complexity (Østvand et al., 2014). The high-end inertia for the CO_2-response is also more consistent with complex Carbon-cycle models, and the long-memory nature

5   of the residual Mauna Lua record, as shown in Fig. 2d.

3.4   Policy implications

The range of the projections corresponding to given emission scenarios presented in Fig. 5a–d is much wider than the uncertainty of scientific knowledge reflected in the climate science literature. But it may give an indication of the doubts which are quite

10   common outside the climate science community. Among these are the belief that CO_2 is removed from the atmosphere within decades (Solomon, 2008), and that the GMST relaxes to a new radiative equilibrium within a few years after a sudden perturbation of radiative forcing (Schwartz, 2007). Figure 5a presents projections which follow from these perceptions. Interestingly, the unmitigated projections up to AD 2110 (blue curves) are

15   almost identical in all panels in Fig. 5. Hence, the inertia in the responses has little influence on the unmitigated response to the BAU emission scenario and uncertainty about the magnitude of the inertia parameters does not contribute much to uncertainty in the response to this scenario. Uncertainty in these parameters mainly plays a role for the projected effect of the emission reduction after action has been taken, as can be

20   observed by comparing Fig. 5a and d. The effect of emission reduction is considerably greater under the optimistic low-inertia assumptions, but in all circumstances, delayed mitigation action increases the GMST in AD 2200 by 1–2 degrees for every 40 years of delay.

One implication from this observation is that the global warming optimists have little

25   reason for their optimism, since even the projections in Fig. 5a imply that the two-degree climate target will not be attained unless a radical and consistent emission reduction regime is initiated within a few decades from now. If this mitigation regime is delayed and initiated one generation later even the optimistic projections indicate that

the temperature will peak close to 3 degrees during the next century, and postponing yet another generation will let the temperature to rise beyond 4 degrees. If emission reductions are raised to the absolute pain threshold of 5 % per yr, the peak temperature will not change much, but the temperature will come down faster after action has been initiated.

Under the more pessimistic, and presumably more realistic, circumstances presented in Fig. 5b and d the two-degree target is attainable only if extremely radical reductions (5 % per yr) are initiated within the coming two decades. Since such a strong emission reduction regime probably is politically infeasible, this target most likely is unattainable, and the globe will warm 3–7 degrees before the end of next century. Where the GMST will end within this range will essentially depend on the time it takes before radical global emission reductions is implemented. Hence, the slow socio-economic response may turn out to be the most detrimental of all inertia effects which threaten to aggravate global warming.

4   Conclusions

It has been demonstrated that an extremely simple model for the global temperature response and the elimination of excess CO_2 from the atmosphere is all that is needed to make reasonable projections of global temperature under idealised emission scenarios. The model contains only four parameters; characterising sensitivities and inertia in the temperature and CO_2 responses, respectively. All parameters can be estimated from observation data, although some constraining from high-complexity ESMs is useful. The model can be used as a pedagogical tool for students and scientists with some knowledge of elementary calculus, and projections can easily be produced under emissions scenarios different from those presented here.

The simplicity of the model may be perceived as an insult to "real" climate modellers, but as long as one deals only with global quantities, simplicity does not necessarily mean lack of accuracy. Global temperature has been found to respond quite linearly to

forcing in general circulation models (Meehl et al., 2004), and as long as the climate system is far from a major tipping point, this linearity may also pertain to the response of atmospheric CO_2 content to emissions. Under linearity and stationarity assumptions these two quantities are fully described in terms of their respective response functions, whose form can be postulated from basic physical principles and parameters estimated from observation.

For the policy makers of the world it is crucial to know to what extent an economically and politically painful mitigation scenario can be expected to be effective in constraining global warming. The analysis presented here confirms the main conclusion drawn by Stocker (2013); the greatest threat against the stability of the global climate is the inability of humankind to respond in time.

The Supplement related to this article is available online at doi:10.5194/esdd-6-1789-2015-supplement.

References

Allen, M. R., Frame, D. J., Huntingford, C., Jones, C. D., Lowe, J. A., Meinshausen, M., and Meinshausen, N.: Warming caused by cumulative carbon emissions towards the trillionth tonne, Nature, 458, 1163–1166, doi:10.1038/nature08019, 2009. 1791

Anderegg, W. R. L., Prall, J. W., Harold, J., and Schneider, S. H.: Expert credibility in climate change, P. Natl. Acad. Sci. USA, 107, 12107–12109, doi:10.1073/pnas.1003187107, 2010. 1790

Beran, J.: Statistics for Long-memory Processes, Monographs on Statistics and Applied Probability, Chapman and Hall/CRC, Boca Raton, 1994. 1795

Inertia in the climate response

K. Rypdal

Brohan, P., Kennedy, J. J., Harris, I., Tett, S. F. B., and Jones, P. D.: Uncertainty estimates in regional and global observed temperature changes: A new data set from 1850, J. Geophys. Res., 111, D12106, doi:10.1029/2005JD006548, 2006. 1796

Budyko, M. I.: The effect of solar radiation variations on the climate of the Earth, Tellus, 21, 611–619, doi:10.1111/j.2153-3490.1969.tb00466.x, 1969. 1794

Cook, J., Nucitelli, D., Green, S. A., Richardson, M., Winkler, B., Painting, R., Way, R., Jacobs, P., and Skuce, A.: Quantifying the consensus on anthropogenic global warming in the scientific literature, Environ. Res. Lett., 8, 024024, doi:10.1088/1748-9326/8/2/024024, 2013. 1790

den Elzen, M., Meinshausen, M., and van Vuuren, D.: Multi-gas emission envelopes to meet greenhouse gas concentration targets: costs versus certainty of limiting temperature increase, Global Environ. Change, 17, 260–280, doi:10.1016/j.gloenvcha.2006.10.003, 2007. 1801

Geoffroy, O., Saint-Martin, D., Olivié, D. J. L., Voldoire, A., Bellon, G., and Tytcá, S.: Transient climate response in a two-layer energy-balance model. Part I: Analytical solution and parameter calibration using CMIP5 AOGCM experiments, J. Climate, 6, 1841–1857, doi:10.1175/JCLI-D-12-00195.1, 2013. 1795

Hansen, J., Sato, M., Kharecha, P., and von Schuckmann, K.: Earth's energy imbalance and implications, Atmos. Chem. Phys., 11, 13421–13449, doi:10.5194/acp-11-13421-2011, 2011. 1796, 1797

Joos, F., Roth, R., Fuglestvedt, J. S., Peters, G. P., Enting, I. G., von Bloh, W., Brovkin, V., Burke, E. J., Eby, M., Edwards, N. R., Friedrich, T., Frölicher, T. L., Halloran, P. R., Holden, P. B., Jones, C., Kleinen, T., Mackenzie, F. T., Matsumoto, K., Meinshausen, M., Plattner, G.-K., Reisinger, A., Segschneider, J., Shaffer, G., Steinacher, M., Strassmann, K., Tanaka, K., Timmermann, A., and Weaver, A. J.: Carbon dioxide and climate impulse response functions for the computation of greenhouse gas metrics: a multi-model analysis, Atmos. Chem. Phys., 13, 2793–2825, doi:10.5194/acp-13-2793-2013, 2013. 1798, 1799, 1810

Le Quéré, C., Moriarty, R., Andrew, R. M., Peters, G. P., Ciais, P., Friedlingstein, P., Jones, S. D., Sitch, S., Tans, P., Arneth, A., Boden, T. A., Bopp, L., Bozec, Y., Canadell, J. G., Chini, L. P., Chevallier, F., Cosca, C. E., Harris, I., Hoppema, M., Houghton, R. A., House, J. I., Jain, A. K., Johannessen, T., Kato, E., Keeling, R. F., Kitidis, V., Klein Goldewijk, K., Koven, C., Landa, C. S., Landschützer, P., Lenton, A., Lima, I. D., Marland, G., Mathis, J. T., Metzl, N.,

Title Page

Abstract | Introduction

Conclusions | References

Tables | Figures

|◀ | ▶|

◀ | ▶

Back | Close

Full Screen / Esc

Printer-friendly Version

Interactive Discussion

Nojiri, Y., Olsen, A., Ono, T., Peng, S., Peters, W., Pfeil, B., Poulter, B., Raupach, M. R., Regnier, P., Rödenbeck, C., Saito, S., Salisbury, J. E., Schuster, U., Schwinger, J., Séférian, R., Segschneider, J., Steinhoff, T., Stocker, B. D., Sutton, A. J., Takahashi, T., Tilbrook, B., van der Werf, G. R., Viovy, N., Wang, Y.-P., Wanninkhof, R., Wiltshire, A., and Zeng, N.: Global carbon budget 2014, Earth Syst. Sci. Data, 7, 47–85, doi:10.5194/essd-7-47-2015, 2015. 1799

Matthews, H. D., Gilett, N. P., Stott, P. A., and Zickfeld, K.: The proportionality of global warming to cumulative carbon emissions, Nature, 459, 1129–132, doi:10.1038/nature08047, 2009. 1791

Meehl, G. A., Washington, W. M., Amman, C. M., Arblaster, J. M., Wigley, T. M., and Tebaldi, C.: Combinations of Natural and Anthropogenic Forcings in Twentieth-Century Climate, J. Climate, 17, 3721–3727, 2004. 1793, 1805

Meinshausen, M., Smith, S. J., Calvin, K., Daniiel, J. S., Kainuma, M. L. T., Lamarque, J.-F., Matsumoto, K., Montzka, S. A., Raper, S. C. B., Riahi, K., Thomson, A., Velders, G. J. M., and van Vuuren, D. P. P.: The RCP greenhouse gas concentrations and their extensions from 1765 to 2300, Climatic Change, 11, 2013–241, doi:10.1007/s10584-011-0156-z, 2011. 1796, 1797, 1802

Myhre, G., Highwood, J., Shine, K. P., and Stordahl, F.: New estimates of radiative forcing due to well-mixed greenhouse gases, Geophys. Res. Lett., 25, 2715–2718, 1998. 1800

Østvand, L., Nilsen, T., Rypdal, K., Divine, D., and Rypdal, M.: Long-range memory in internal and forced dynamics of millennium-long climate model simulations, Earth Syst. Dynam., 5, 295–308, doi:10.5194/esd-5-295-2014, 2014. 1795, 1803

Rypdal, K.: Global temperature response to radiative forcing: solar cycle versus volcanic eruptions, J. Geophys. Res., 117, D06115, doi:10.1029/2011JD017283, 2012. 1794, 1797

Rypdal, K., Østvand, L., and Rypdal, M.: Long-range memory in Earth's surface temperature on time scales from months to centuries, J. Geophys. Res., 118, 7046–7062, doi:10.1002/jgrd.50399, 2013.

Rypdal, K., Rypdal, M., and Fredriksen, H.-B.: Spatiotemporal Long-Range Persistence in Earth's temperature field: analysis of stochastic-diffusive energy balance models, J. Climate, in press, 2015. 1795, 1803

Rypdal, M. and Rypdal, K.: Long-memory effects in linear-response models of Earth's temperature and implications for future global warming, J. Climate, 27, 5240–5258, doi:10.1175/JCLI-D-13-00296.1, 2014. 1794, 1795

Title Page

Abstract | Introduction

Conclusions | References

Tables | Figures

◄ | ►

◄ | ►

Back | Close

Full Screen / Esc

Printer-friendly Version

Interactive Discussion

Schwartz, S. E.: Heat capacity, time constant, and sensitivity of the Earth's climate system, J. Geophys. Res., 112, D24S05, doi:10.1029/2007JD008746, 2007. 1803

Sellers, W. D.: A global climate model based on the energy balance of the Earth-atmosphere system, J. Appl. Meteorol., 8, 392–400, 1969. 1794

5 Solomon, L.: The Deniers. The World-Renowned Scientists Who Stood Up Against Global Warming Hysteria, Political Persecution and Fraud, Richard Viglante Books, USA, 2008. 1801, 1803

Stocker, T. F.: The closing door of climate targets, Science, 339, 280–282, doi:10.1126/science.1232468, 2013. 1791, 1792, 1801, 1805

10 Stocker, T. F., Qin, D., Plattner, G.-K., Tignor, M., Allen, S. K., Boschung, J., Nauels, A., Xia, Y., Bex, V., and Midgley, P. M. (Eds.): IPCC, 2013: Climate Change 2013: The Physical Science Basis, in: Contribution of Working Group I to the Fifth Assessment Report of the Intergovernmental Panel on Climate Change, Cambridge University Press, Cambridge, UK and New York, NY, USA, 1535 pp., 2013. 1791, 1793

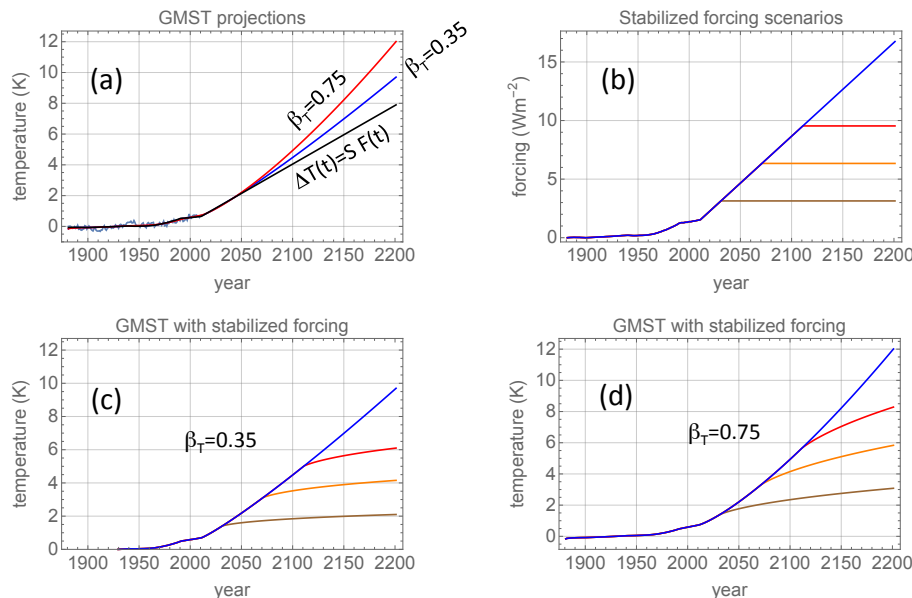15 Stern, N.: The Economics of Climate Change, The Stern Review, Cambridge, 2007. 1801

Figure 1. **(a)** Light blue curve is the instrumental GMST for AD 1880–2010. Black curve is the instantaneous response to the linearly extrapolated forcing scenario shown in **(b)**. Blue curve is the response according to the model Eq. (2) with $\beta_T = 0.35$, and the red curve with $\beta_T = 0.75$. **(b)** The blue curve is a linearly projected forcing to AD 2200 with the same mean growth rate as the the RCP8.5 scenario in the period AD 2010–2100. The brown curve is the stabilisation of this forcing in AD 2030, the blue curve in AD 2070, and the red curve in AD 2110. **(c)** GMST responses to the forcing scenarios in **(b)** with $\beta_T = 0.35$. Colours correspond to those in **(b)**. **(d)** Same as in **(c)**, but with $\beta_T = 0.75$.
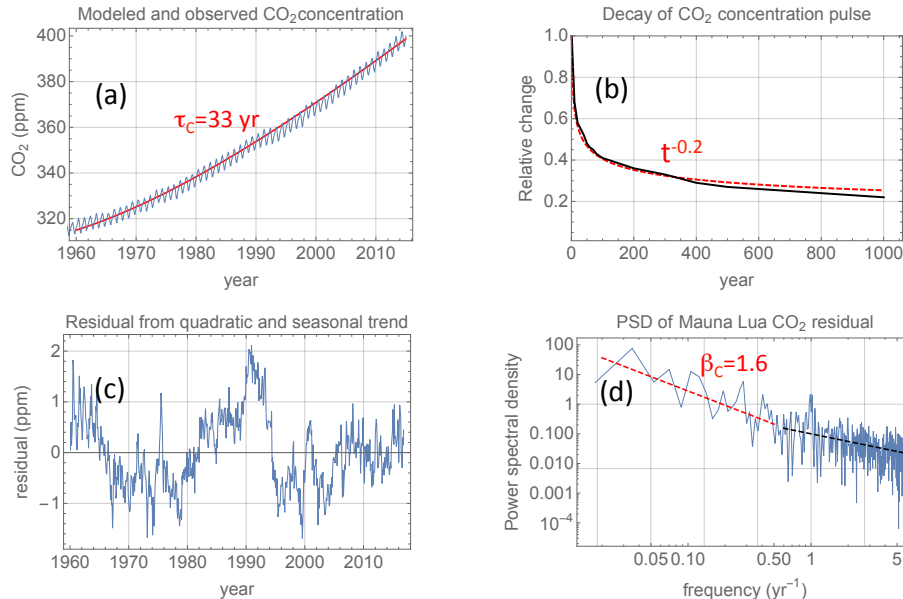
Figure 2. (a) Blue curve shows the atmospheric CO_2 concentration as measured by the Mauna Lua observatory. The red curve is the concentration computed from Eq. (5) with $\tau_C = 33\,\mathrm{yr}$, $\Delta C_{1960} = 74\,\mathrm{Gt\,C}$ (corresponding to an anomaly of $315 - 280 = 35\,\mathrm{ppm}$), and $C_0 = 594\,\mathrm{Gt\,C}$ (corresponding to 280 ppm). **(b)** Black curve is the multimodel mean CO_2 response to a pulse of emitted CO_2 as given in Joos et al. (2013). The red, dashed curve is a least-square fit of a function of the form $\alpha_C t^{\beta_C/2-1}$ with the estimated $\beta_C \approx 1.6$. **(c)** The residual Mauna Lua signal after subtracting the quadratic polynomial and seasonal trends. **(d)** The power spectral density of the residual in **(c)** estimated by the periodogram presented in a log-log plot. The blue, dashed line has negative slope $\beta_C = 0.85$, and the red, dashed line $\beta_C = 1.6$.

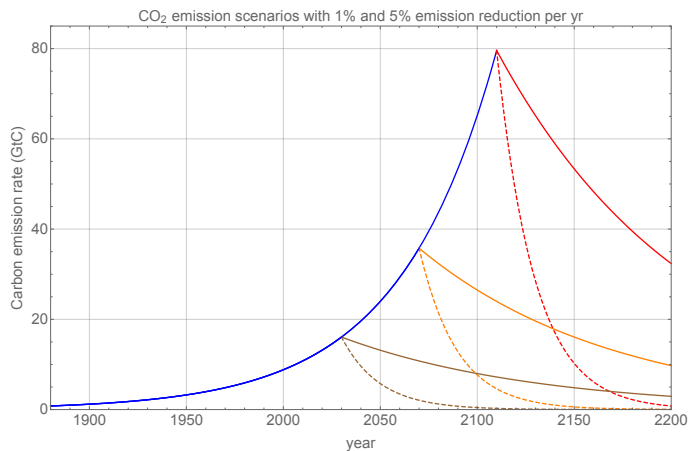**Figure 3.** Blue curve is carbon emission rate $R(t)$ scenario obtained by fitting the exponential $S_0 \exp(gt)$ to the emission rate $4\,\mathrm{Gt\,C\,yr}^{-1}$ in 1960 and $11\,\mathrm{Gt\,C\,yr}^{-1}$ in AD 2010. The full, brown, orange, and red curves are the subsequent $R(t)$ after initiation of $1\,\%$ reduction of emission rate per year. The dashed curves are the corresponding rates with $5\,\%$ reduction per year.

Full Screen / Esc

Printer-friendly Version
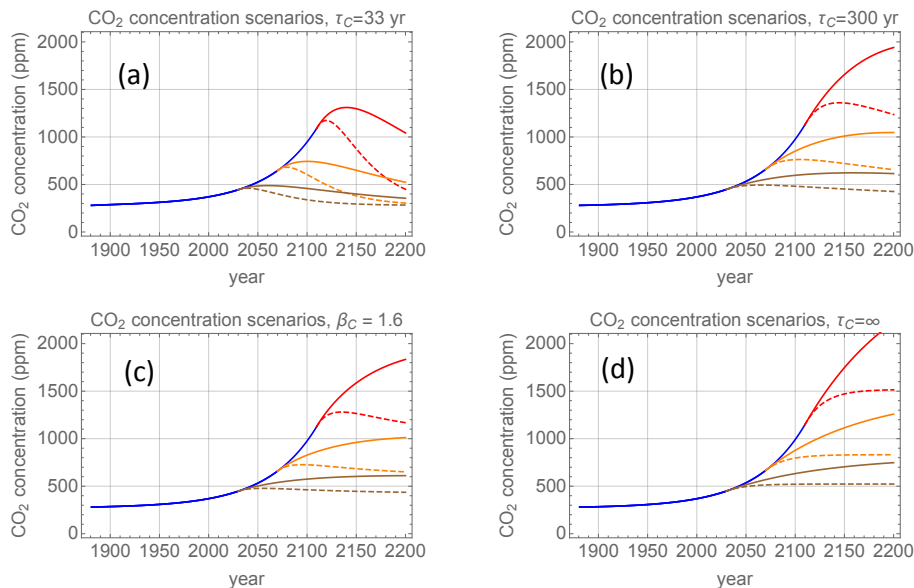
Interactive Discussion

Figure 4. Projections of CO_2 concentration under the emission scenarios in Fig. 3 using the modelling explained in Sect. 2. The colours correspond to those in Fig. 3. **(a)** $\tau_C = 33$ yr, **(b)** $\tau_C = 300$ yr, **(c)** $\beta_C = 1.6$ and **(d)** $\tau_C = \infty$.
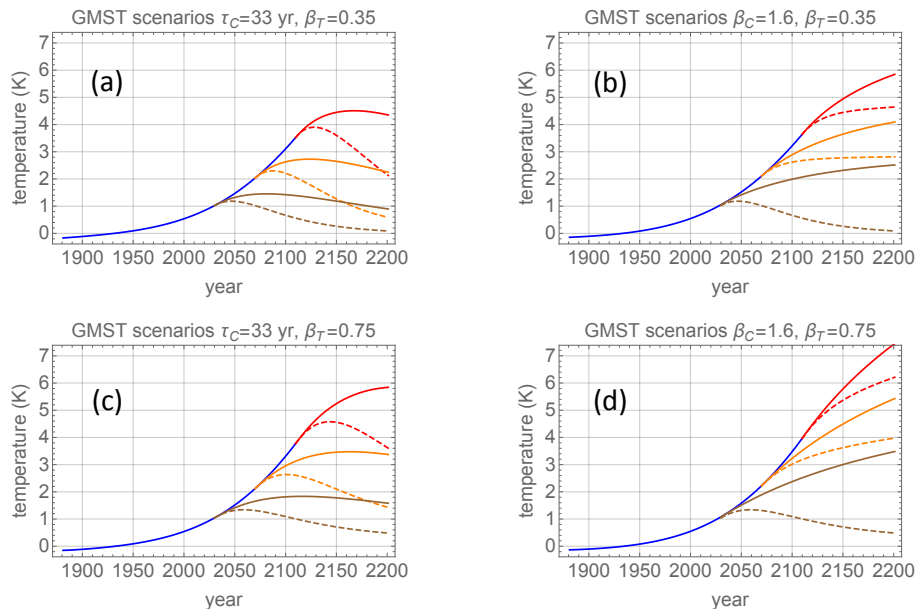
Figure 5. (a) The evolution of the GMST for the CO_2 concentration scenarios shown in Fig. 4a and c. **(a)** $\tau_C = 33$ yr and $\beta_T = 0.35$; **(b)** $\beta_C = 1.6$ and $\beta_T = 0.35$; **(c)** $\tau_C = 33$ yr and $\beta_T = 0.75$ and **(d)** $\beta_C = 1.6$ and $\beta_T = 0.75$.